Supplementary Information (SI) for Journal of Materials Chemistry C.

Supplementary Information

Grain Boundary Effect Unveiled in Monolayer MoS_2 for Photonic Neuromorphic Application

*Navaneeth Krishnan K, Sandaap Sathyanarayana, and Bikas C. Das**

eNDR Laboratory, School of Physics, IISER Thiruvananthapuram, Trivandrum 695551, Kerala, India.

*Email of Corresponding Author: bikas@iisertvm.ac.in

(i)

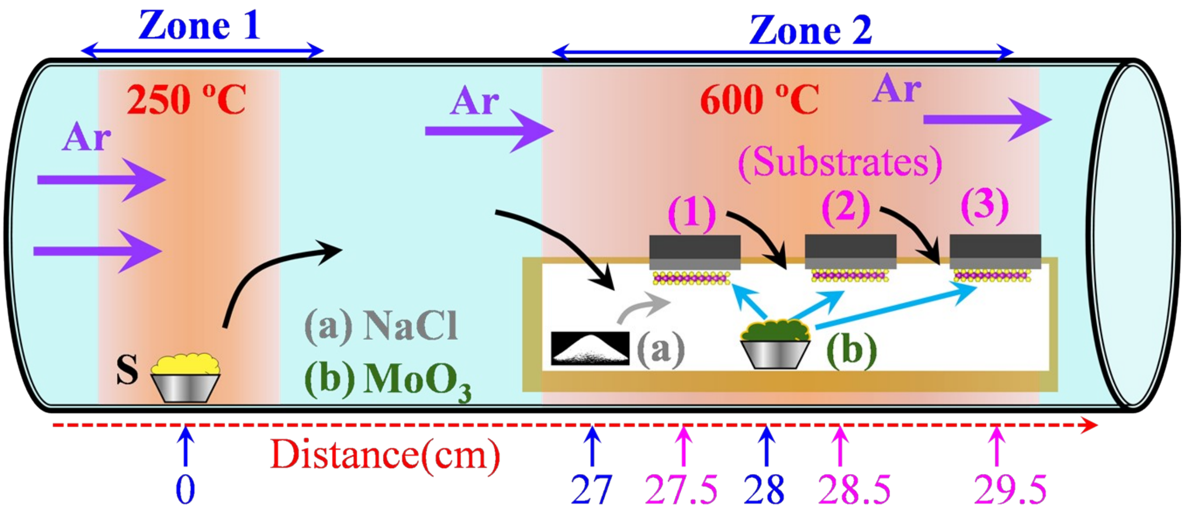

$$3MoO_3\,(s) + 2NaCl\,(s) \longrightarrow Na_2Mo_2O_7\,(l) + MoO_2Cl_2\,(g)$$

$$Na_2Mo_2O_7\,(l) + 7S\,(g) \longrightarrow 2MoS_2\,(s) + Na_2SO_3\,(s) + 2SO_2\,(g)$$

(ii)

Figure S1. (i) This schematic illustrates the alkali halide assisted chemical vapor deposition process of MoS_2 using MoO_3 and S as precursors, with NaCl acting as a seeding promoter at 600 °C. Positions (1), (2), and (3) denote different substrate placements, positioned at distances of 27.5 cm, 28.5 cm, and 29.5 cm downstream from the sulfur (S) precursor located at 0 cm, while NaCl is situated 1.0 cm upstream of the MoO_3 precursor. The equations depict the MoS_2 growth steps inside the CVD chamber. (ii) Optical microscope images show 2D monolayer MoS_2 samples of different shapes at positions (1), (2), and (3) respectively.

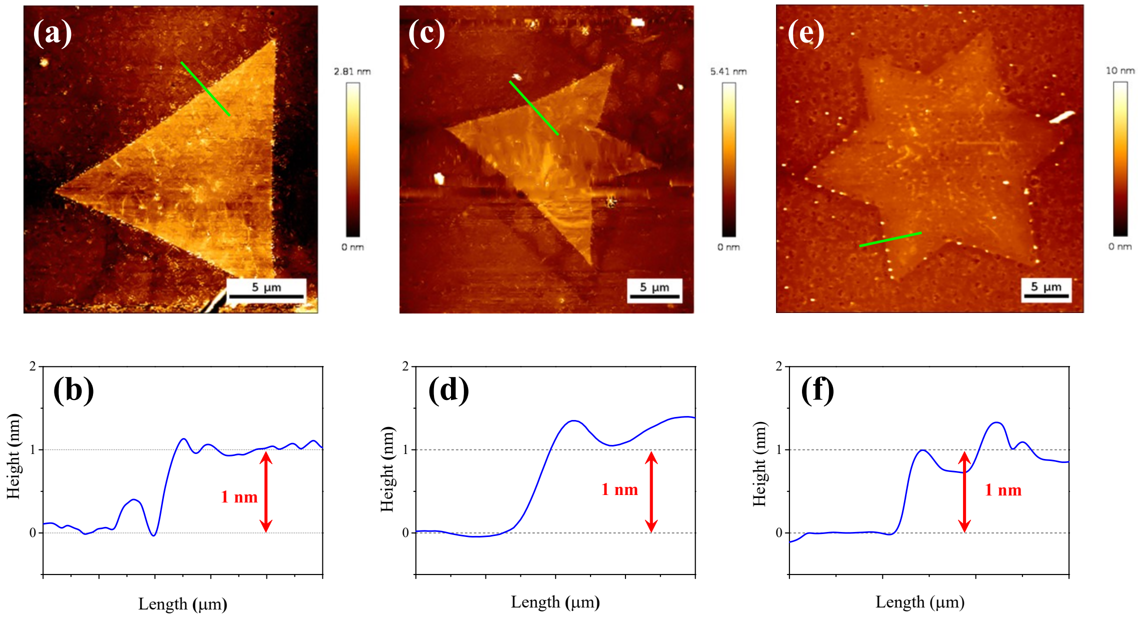

Figure S2. Atomic force microscopy was utilized to capture topographic images of monolayer MoS_2 samples with varying shapes recorded immediately after the growth, alongside the corresponding height profiles extracted along marked lines. Specifically, (a and b) depict triangular shapes, (c and d) showcase four-point star samples, and (e and f) illustrate six-point star samples. The presence of white spots represent the unreacted precursors and/or seeding promoter NaCl, which are removed using focused ion beam (FIB) after device fabrication.

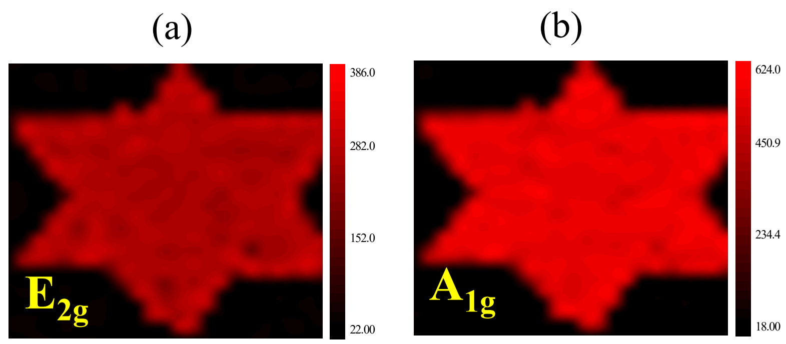

Figure S3. Raman mapping images of six-point star ML MoS_2 sample with 532 nm laser excitation. (a) Depicts in-plane (E^1_{2g}) vibrations and (b) Shows the out-of-plane (A_{1g}) vibrations.

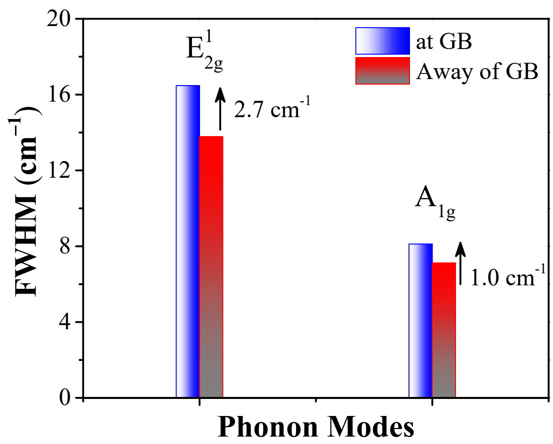

Figure S4. The variation in full-width half-maxima (FWHM) for the E^1_{2g} and A_{1g} phonon modes between the vicinity of the grain boundary (GB) and regions farther from it, as illustrated in Figure 2(a) of the main manuscript.

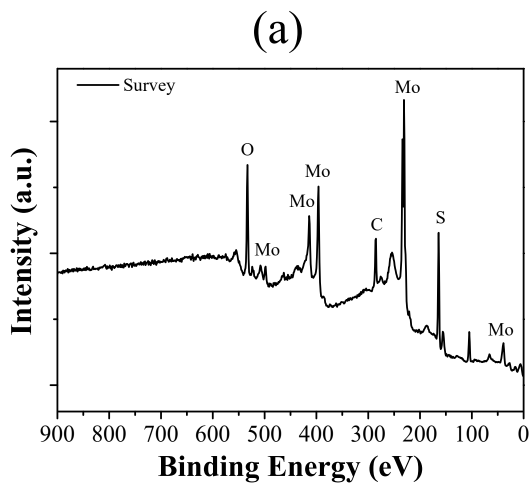

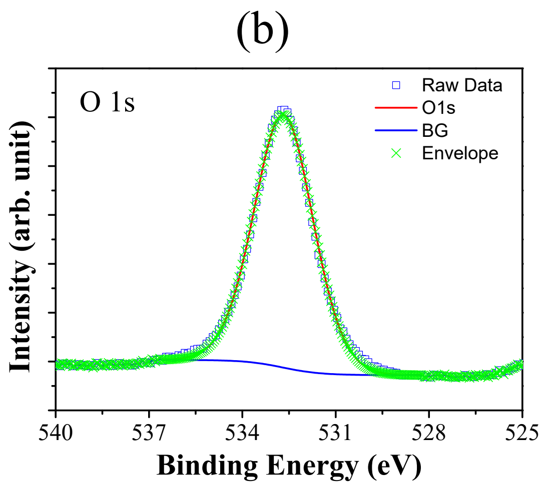

Figure S5. (a) XPS survey spectrum of the CVD grown six-point star ML MoS_2 sample. (b) High-resolution spectral line of O 1s electrons originating from the substrate Si/SiO_2.

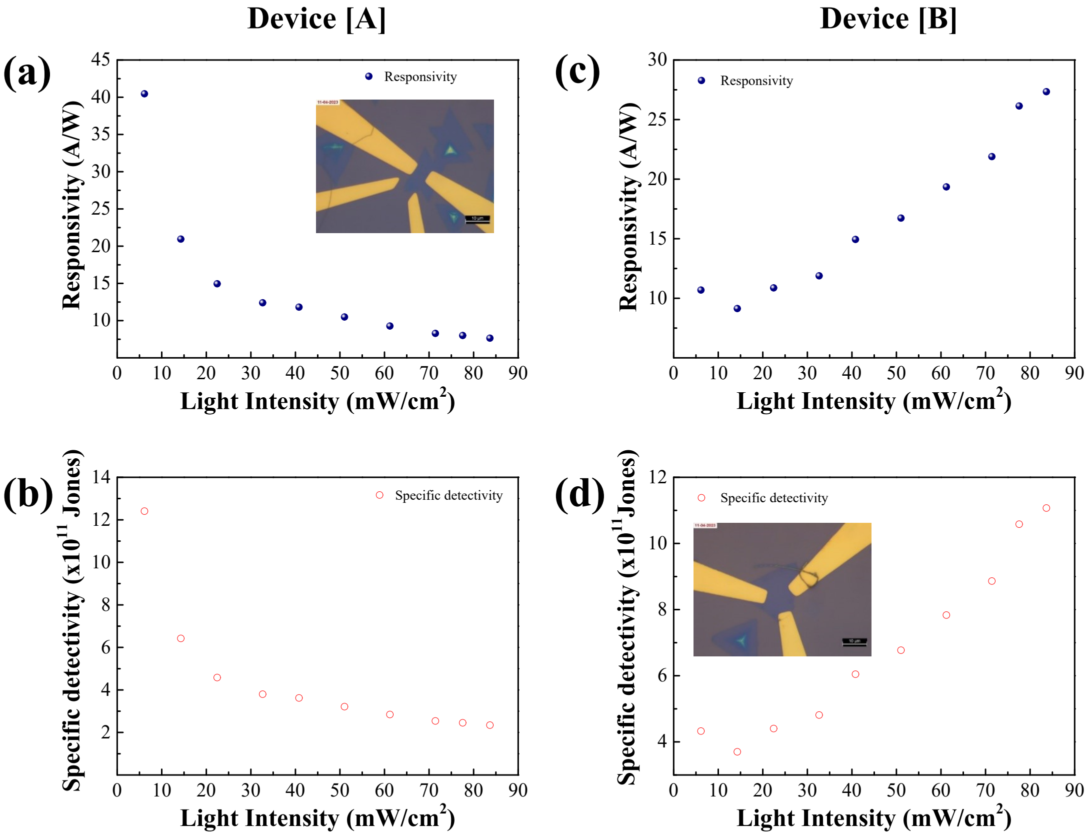

Figure S6. (a and b) Light intensity dependent R and D* for the device [A]. (c and d) Light intensity dependent R and D* for the device [B]. Insets show the opical microscope images of the corresponding devices.

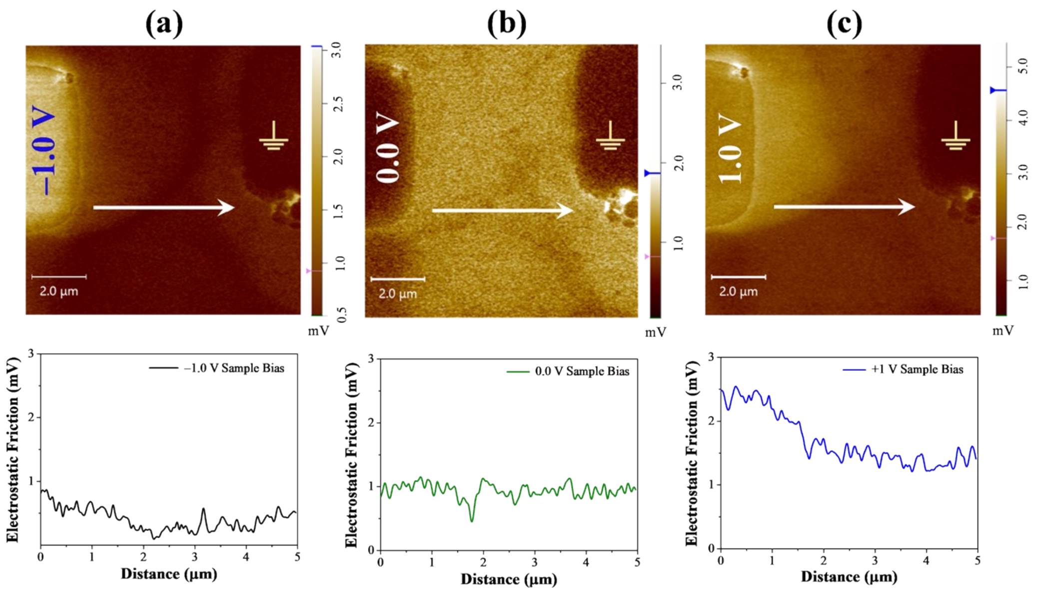

Figure S7. Electrostatic force microscopy (EFM) was employed to map the surface potential of device [A] under light illumination, using different biasing polarities. (a) A biasing voltage of –1.0 V was applied, (b) no biasing voltage was applied, and (c) +1.0 V was applied during scanning. The corresponding line profiles along the marked arrow line reveal that the electrostatic friction, represented by the mV potential unit, is higher when +1.0 V is applied compared to 0 V biasing, and lower when –1.0 V is applied compared to 0 V biasing.

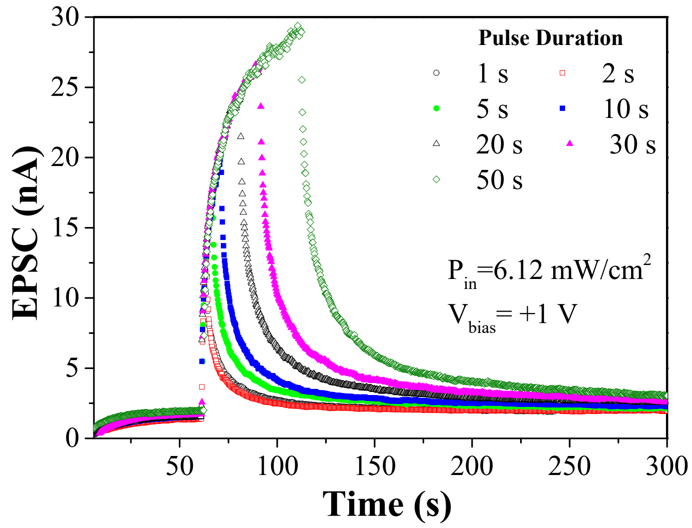

Figure S8. Normalized EPSC responses were obtained by adjusting the width of the light pulses, while maintaining a constant power density of 6.12 mW/cm².

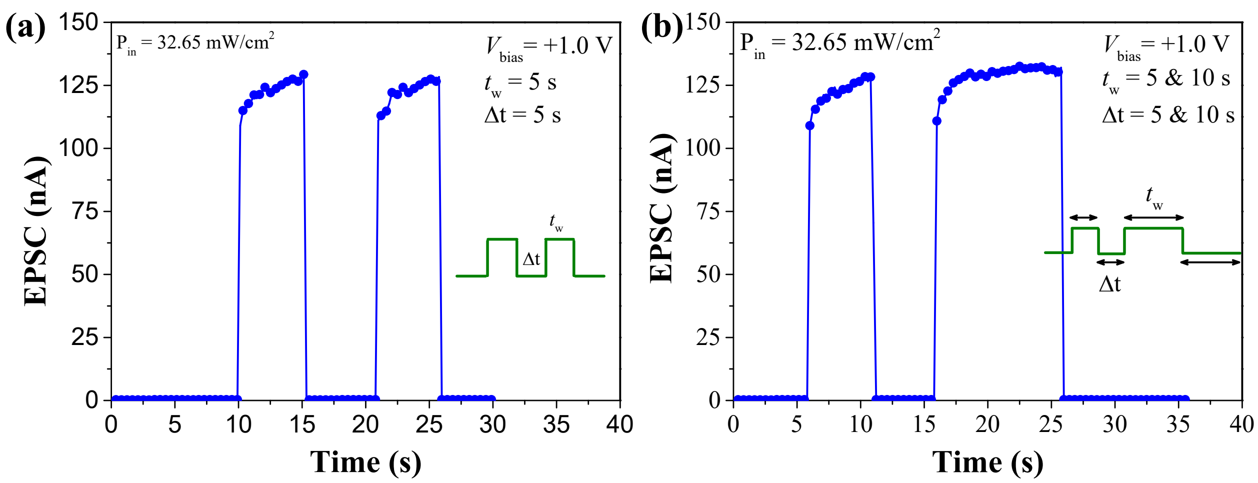

Figure S9. Measurements of Paired Pulse Facilitation (PPF) for device [B] involved employing a pair of light pulses with a power density of 32.65 mw/cm2 and an applied bias of +1.0 V. This was carried out in two scenarios: (a) maintaining a pulse width (tw) and temporal gap (Δt) of 5 s, and (b) utilizing two consecutive pulses with pulse widths (tw) of 5 s and 10 s, respectively, while keeping the temporal gap (Δt) constant at 5 s.

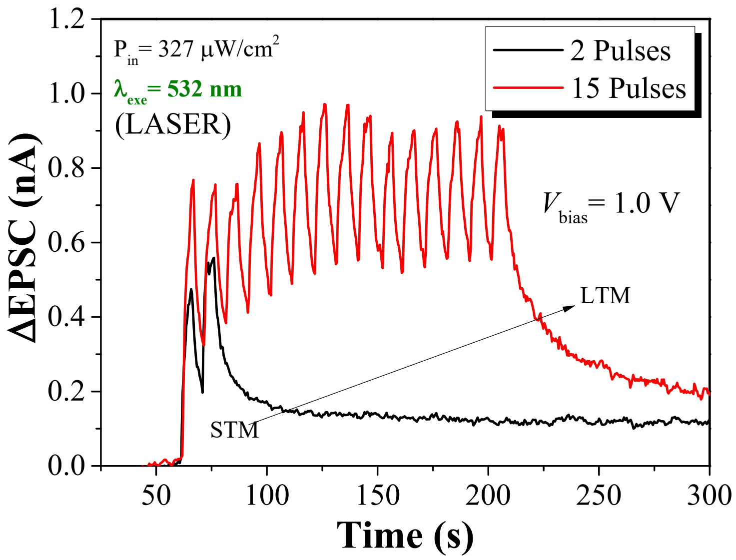

Figure S10. By utilizing sequential laser light pulses (λ= 532 nm, Pin= 327 μW/cm^2) lasting 5 s each, with a temporal gap of 5 s between pulses, we aim to demonstrate synaptic weight potentiation (P) through rehearsal via photonic modulation of EPSC.

Section S1: Photodetector Figure of Merit (FOM) Calculations

The figure of merits (FOM) of a photodetector are responsivity (R), specific detectivity (D*), signal to noise ratio (SNR), noise equivalent power (NEP) and detectivity (D) and they are defined as follows,

a) Responsivity (R)

Responsivity is the ratio of the photocurrent (I_{ph}) to the incident optical power and is expressed in A/W.[1, 2]

$$R = \frac{I_{ph}}{(P_{light}A_{effe})} \tag{1}$$

Where, I_{ph}=I_{light}-I_{dark}, I_{light} is the current under light illumination and I_{dark} is the dark current. A_{effe} is the effective area of the device and P_{light} is the optical power density.

b) Specific detectivity (D*)

The ability to identify the lowest optical signals is characterized as specific detectivity (D*). Given the assumption that shot noise from the dark current accounts for the majority of the total noise, then the D* can be found as follows and it is expressed in cm $Hz^{1/2}W^{-1}$(Jones).[3]

$$D^* = \frac{R\sqrt{A_{effe}}}{\sqrt{(2eI_{dark})}} \qquad (2)$$

Where, R is the responsivity of the photodetector.

c) Signal to Noise Ratio (SNR)

The ratio of signal power to noise power in a photodetector is referred to as the signal to noise ratio. It is expressed as follows:[2]

$$SNR = \frac{Signal\ power}{Noise\ power}$$

$$SNR = \frac{< i_{ph}^2 >}{< i_{noise}^2 >} \qquad (3)$$

d) Noise Equivalent Power (NEP) and Detectivity (D)

The minimal incident radiation power required to achieve SNR of 1 in a 1 Hz bandwidth is known as noise equivalent power. Typically, it is expressed as $WHz^{-1/2}$. It is determined as

$$NEP = \frac{\sqrt{< i_{noise}^2 >}}{R} \qquad (4)$$

Where R is the responsivity and $< i_{noise}^2 >$ is the mean square noise current is the sum of shot noise current ($< i_{sh}^2 >$) and thermal noise current ($< i_{th}^2 >$), they are depending on the bandwidth (B) of the photodetector and described as,

$$Shot\ noise,\ < i_{sh}^2 > \ = 2qB < i_d > \qquad (5)$$

$$Thermal\ noise,\ < i_{th}^2 > \ = \frac{4kTB}{r} \qquad (6)$$

By substituting equation (5) and (6) in (4) as

$$NEP = \frac{\sqrt{< i_{sh}^2 > + < i_{th}^2 >}}{R} \qquad (7)$$

$$NEP = \frac{\sqrt{2qB < i_d > \ + \ \frac{4kTB}{r}}}{R} \qquad (8)$$

Where, B is the bandwidth of the photodetector which is given by $B = \frac{0.35}{\tau_{rise}}$, q is the electronic charge, τ_{rise} is the rise time of the photodetector, $< i_d >$ is average dark current obtained from the temporal response of the device, kT is the thermal energy and r is the resistance of the device and is given by $r = \frac{V}{I_{dark}}$.[2]

For an entire bandwidth (B), NEP is expressed in W and the reciprocal of the NEP is given by the detectivity (D) of the photodetector and is expressed in W^{-1}.[2]

By considering the above mentioned equations, Device [A] and Device [B] figure of merits are found as below.

For Device A:

From the temporal response of the device given in main manuscript, the average dark current is

$< i_d >= 1.36631 \times 10^{-9} A$

From the temporal response the rise time of the Device [A] is 12.88 s, therefore the bandwidth is given by $B = \frac{0.35}{\tau_{rise}} = 27.1\ mHz$.

By substituting the values in equation (5),

$< i_{sh}^2 > \ = 2qB < i_d > \ = 1.1881 \times 10^{-29} A^2$

The resistance (r) of the Device [A] is given by $r = \frac{V}{I_{dark}}$ =0.899 GΩ, where I_{dark}=1.112 nA at 1 V applied bias.

The signal power that is square mean of the photocurrent, obtained from the temporal response of the Device [A] is

$< i_{ph}^2 > \ = 3.5853 \times 10^{-14} A^2$

The calculated thermal noise by substituting the values of B, r, kT in equation (6) is $< i_{th}^2 >= 5.00883 \times 10^{-31} A^2$.

By adding the shot noise and thermal noise power will give the total noise power i.e.

$< i_{noise}^2 >= 1.23818 \times 10^{-29} A^2$

Therefore the signal to noise ratio is,

$$SNR = \frac{< i_{ph}^2 >}{< i_{noise}^2 >} = 2.8956 \times 10^{15} = 154.462\ dB$$

The Responsivity and Specific detectivity are estimated for Device [A] at different light intensities as shown in Table S1.

Table S1: Variation of Responsivity and Specific detectivity with a function of light intensity for device [A].

Intensity (mW/cm^2)	**R (A/W)**	**D* × 10^{11} (Jones)**
6.12	40.5	12.4
12.49	20.9	6.42
22.45	14.9	4.58
32.65	12.4	3.80
40.82	11.8	3.62
51.02	10.5	3.21
61.22	9.27	2.84
71.43	8.28	2.54
77.55	8.00	2.45
83.67	7.64	2.34

The NEP (for bandwidth 1 Hz) and NEP (for entire bandwidth) are estimated for Device [A] at different light intensities as shown in Table S2. The detectivity (D) is the reciprocal of NEP (for entire bandwidth) also included in Table S2.

Table S2: NEP for B of 1 Hz, for entire bandwidth and detectivity of Device [A]

Intensity (mW/cm^2)	**NEP ($W/\sqrt{Hz}$)**	**NEP (W)**	**Detectivity (W^{-1})**
6.12	5.27×10^{-16}	8.69×10^{-17}	1.15×10^{16}
12.49	1.02×10^{-15}	1.68×10^{-16}	5.94×10^{15}
22.45	1.43×10^{-15}	2.36×10^{-16}	4.23×10^{15}

32.65	1.72×10^{-15}	2.84×10^{-16}	3.52×10^{15}
40.82	1.81×10^{-15}	2.98×10^{-16}	3.35×10^{15}
51.02	2.03×10^{-15}	3.35×10^{-16}	2.98×10^{15}
61.22	2.30×10^{-15}	3.80×10^{-16}	2.63×10^{15}
71.43	2.58×10^{-15}	4.25×10^{-16}	2.35×10^{15}
77.55	2.67×10^{-15}	4.40×10^{-16}	2.27×10^{15}
83.67	2.79×10^{-15}	4.61×10^{-16}	2.17×10^{15}

For Device B:

From the temporal response of the device given in main manuscript, the average dark current is $< i_d >= 2.86538 \times 10^{-10} A$

From the temporal response the rise time of the Device [A] is 256 ms, therefore the bandwidth is given by $B = \frac{0.35}{\tau_{rise}} = 1.3671\ Hz$.

By substituting the values in equation (5),

$< i_{sh}^2 > \ = 2qB < i_d > \ = 1.25352 \times 10^{-28} A^2$

The resistance (r) of the Device [A] is given by $r = \frac{V}{I_{dark}}$ =1.234 GΩ, where I_{dark} = 0.8102 nA at 1V applied bias.

The signal power that is square mean of the photocurrent, obtained from the temporal response of the Device [A] is

$< i_{ph}^2 > \ = 1.78478 \times 10^{-14} A^2$

The calculated thermal noise by substituting the values of B, r, kT in equation (6) is $< i_{th}^2 >= 1.83869 \times 10^{-29} A^2$.

By adding the shot noise and thermal noise power will give the total noise power i.e.,

$< i_{noise}^2 >= 1.43716 \times 10^{-28} A^2$

Therefore the signal to noise ratio is,

$$SNR = \frac{< i_{ph}^2 >}{< i_{noise}^2 >} = 1.24188 \times 10^{14} = 140.94\ dB$$

The Responsivity and Specific detectivity are estimated for Device [B] at different light intensities as shown in Table S3.

Table S3: Variation of Responsivity and Specific detectivity with a function of light intensity for the device [B].

Intensity (mW/cm^2)	**R (A/W)**	**D* (Jones)**
6.12	10.7	4.33×10^{11}
12.49	9.14	3.70×10^{11}
22.45	10.9	4.40×10^{11}
32.65	11.9	4.81×10^{11}
40.82	14.9	6.05×10^{11}
51.02	16.7	6.77×10^{11}
61.22	19.3	7.83×10^{11}
71.43	21.9	8.86×10^{11}
77.55	26.1	1.06×10^{12}
83.67	27.3	1.11×10^{12}

The NEP (for bandwidth 1 Hz) and NEP (for entire bandwidth) are estimated for Device [B] at different light intensities as shown in Table S4. The detectivity (D) is the reciprocal of NEP (for entire bandwidth) also included in Table S4.

Table S4: NEP for B of 1 Hz, for entire bandwidth and detectivity of Device [B]

Intensity (mW/cm^2)	**NEP ($W/\sqrt{Hz})$**	**NEP (W$)$**	**Detectivity (W^{-1})**
6.12	9.58×10^{-16}	1.12×10^{-15}	8.92×10^{14}
12.49	1.12×10^{-15}	1.31×10^{-15}	7.62×10^{14}
22.45	9.41×10^{-16}	1.10×10^{-15}	9.09×10^{14}

32.65	8.62×10^{-16}	1.01×10^{-15}	9.92×10^{14}
40.82	6.88×10^{-16}	8.05×10^{-15}	1.24×10^{15}
51.02	6.14×10^{-16}	7.18×10^{-16}	1.39×10^{15}
61.22	5.31×10^{-16}	6.21×10^{-16}	1.61×10^{15}
71.43	4.68×10^{-16}	5.48×10^{-16}	1.83×10^{15}
77.55	3.93×10^{-16}	4.59×10^{-16}	2.18×10^{15}
83.67	3.76×10^{-16}	4.39×10^{-16}	2.28×10^{15}

Supporting References:

(1) Tamalampudi, S. R.; Lu, Y. Y.; Kumar, U. R.; Sankar, R.; Liao, C. D.; Moorthy, B. K.; Cheng, C. H.; Chou, F. C.; Chen, Y. T. High Performance and Bendable Few-Layered InSe Photodetectors with Broad Spectral Response. *Nano Letters* **2014**, *14* (5), 2800-2806.

(2) Wang, F., Zhang, T., Xie, R. *et al.* How to characterize figures of merit of two-dimensional photodetectors. *Nat Commun* **2023,** *14* (2224).

(3) Wang, F.; Wang, Z. X.; Yin, L.; Cheng, R. Q.; Wang, J. J.; Wen, Y.; Shifa, T. A.; Wang, F. M.; Zhang, Y.; Zhan, X. Y.; et al. 2D library beyond graphene and transition metal dichalcogenides: a focus on photodetection. *Chemical Society Reviews* **2018**, *47* (16), 6296-6341.